

CONCURRENT MULTI-PARAMETER LEARNING DEMONSTRATED ON THE KURAMOTO-SIVASHINSKY EQUATION.

BENJAMIN PACHEV*, JARED P. WHITEHEAD†, AND SHANE A. MCQUARRIE*

Abstract. We develop an algorithm for the concurrent (on-the-fly) estimation of parameters for a system of evolutionary dissipative partial differential equations in which the state is partially observed. The intuitive nature of the algorithm makes its extension to several different systems immediate, and it allows for recovery of multiple parameters simultaneously. We test this algorithm on the Kuramoto-Sivashinsky equation in one dimension and demonstrate its efficacy in this context.

Key words. Data assimilation, parameter recovery, Kuramoto-Sivashinsky equation, nudging

AMS subject classifications. 35F20, 35R30, 65M32, 65M70

1. Introduction. Every mathematical model has parameters that must be identified correctly to match reality. This is often a difficult task, as such parameters are difficult to measure and/or noise in the measurement process precludes identifying the parameters exactly. Motivated by [9], we develop a robust algorithm that estimates multiple parameters in a partial differential equation (PDE) when those parameters can be written as coefficients of the various terms in the PDE. As the current algorithm relies on the feedback control data assimilation mechanism introduced in [1], we simultaneously identify not only the parameters of the system, but also obtain the dynamical state of the system based on reduced observations of the true state.

The method presented herein differs in important ways from other data-driven parameter recovery or equation discovery methods in the recent literature, the majority of which are *offline* procedures in the sense that they seek to learn models from a previously collected set of training data. The sparse identification of nonlinear dynamical systems (SINDy) framework [7] generates a library of nonlinear candidate functions and leverages sparsity-promoting optimization techniques to generate the model that, as a linear combination of only a few of the candidate functions, best explains a set of observed dynamics. The coefficients of the resulting model are fixed, though some progress has been made toward adaptivity through sparse updates to existing models [39]. Recent advances in deep learning propose neural network models that build the residual of a known governing equation into the training loss function, informing the optimization problem of the desired physics [40]. Other deep learning approaches aim to directly approximate parameter-to-solution operators with neural networks [35, 33], establishing a mapping between system parameters and solutions of the underlying PDEs. Such approaches massively overparameterize the system dynamics, endowing the resulting network with expressivity but at the expense of training efficiency. Bayesian statistics yields yet another framework wherein a posterior distribution with associated uncertainties can be constructed for the parameters of the PDE, or even the solution itself (see [6] for example). The use of Markov Chain Monte Carlo (MCMC) methods in this context provide robust methods for estimating the posterior distribution, and the advantages of the Bayesian approach are multifaceted [14]; however, such analysis is computationally prohibitive at best as even

*Oden Institute for Computational Engineering and Sciences, University of Texas at Austin, Austin, TX (benjaminpachev@gmail.com, shanemcq@utexas.edu).

†Department of Mathematics, Brigham Young University, Provo, UT (whitehead@mathematics.byu.edu).

the most advanced MCMC methods require thousands of evaluations of a numerical approximation to the PDE.

In contrast, the method we propose is a *concurrent* (on-the-fly) procedure, providing updates to the unknown parameters of a target model simultaneous to the assimilation of measurements. We consider the setting in which the form of the governing equations is known, and therefore have no need to construct a (potentially deficient) library of candidate terms or overparametrize the solution representation, although extensions of this approach to settings where less is known about the governing equation are certainly feasible. We leverage well-established methods originally developed to determine the true state of a system when the model is fully known, but in our setting we additionally infer the unknown system parameters.

Our derivation is motivated by the Azouani-Olson-Titi (AOT) [1] algorithm developed for the continuous assimilation of limited data into a known dissipative dynamical system. Since [1], this approach has been adapted to numerous other systems (see [3, 27, 5] for example) and settings in which the observed variables are various subsets of the full system's variables (see [20, 21, 22, 19] for example) or where different types of observations and nudging are utilized (see [32, 4] for example). All of these extensions have broadened the applicability of the AOT algorithm but rely on the accurate representation of the underlying model parameters. Recently, data assimilation for an imperfect model has been considered in different contexts [15, 9, 18]. It is rigorously established for two distinct settings that when a parameter of the system is unknown, that error in the assimilation will still converge up to the error in a single unknown parameter (see [9, 18]). An upcoming article [10] takes these concepts a step further, deriving analogous update formulae for the three parameters of the Lorenz equations [34] and carrying out a thorough numerical investigation to explore the limitations of these formulae. In addition, asymptotic convergence to the true parameter values under suitable conditions is rigorously guaranteed, giving the first instance where a rigorous mathematical framework is available for this approach to learning parameters. We expand on all of this previous work, developing an algorithm that works not only for a single unknown parameter, but for multiple unknowns, and which theoretically applies to any dissipative dynamical system.

The algorithm presented below is derived in a general setting and is applicable to a wide class of dissipative PDEs. Here we examine the efficacy of this algorithm for the Kuramoto-Sivashinsky equation (KSE) numerically. KSE is selected because it presents chaotic spatial-temporal dynamics at a relatively low computational cost (see [43, 13, 8, 16] for example studies of the complicated dynamics that arise in KSE). In addition, KSE naturally provides the context for introducing several artificial parameters whose estimation is of significant import.

KSE has been derived in a variety of contexts, typically as a model for physical systems that are far from equilibrium. The original derivation of KSE was to study instabilities in a reaction diffusion system [30] and simultaneously on the instability and turbulent behavior of a single flame [41]. KSE also appears in the study of plasmas [31, 11], in irregular flow down an inclined plane [42], and it is shown in [36] that KSE provides a general description for part of the dynamical evolution of systems following a certain type of bifurcation point. Mathematically, KSE is often used as an ideal setting to investigate nonlinear dynamics, coherent structures, long-time behavior of solutions, and the testing of methods developed to investigate these properties (see [26, 37, 23, 12, 25, 24] for example). Such earlier works have demonstrated that although KSE is simple and computationally cheap to simulate, it displays a wide variety of interesting dynamics similar to more complicated systems

and is a reasonable testbed for the parameter estimation algorithm proposed below.

This paper is organized as follows. The derivation of the parameter recovery algorithm is presented in [Section 2](#), numerical simulations applied to KSE are presented in [Section 3](#) that demonstrate the apparent numerical properties of the algorithm, and [Section 4](#) draws conclusions and discusses extensions of these results to other systems, and the potential for rigorous justification of the main algorithm.

2. Derivation of the Algorithm. In this section, we develop a parameter recovery algorithm in a general setting. Let $\Omega \subset \mathbb{R}^d$, $d \in \{1, 2, 3\}$, be an open set with Lipschitz continuous boundary $\partial\Omega$, and let $\mathcal{V} = L^2(\Omega)$ with symmetric inner product $\langle \cdot, \cdot \rangle$. Consider a PDE of the form

$$(2.1) \quad \mathbf{u}_t + F(\mathbf{u}) + \sum_{k=1}^n \lambda_k G_k(\mathbf{u}) = \mathbf{f},$$

where $\mathbf{u} = \mathbf{u}(\mathbf{x}, t)$ is an unknown physical quantity (e.g., velocity), $\mathbf{u}_t = \frac{\partial}{\partial t} \mathbf{u}(\mathbf{x}, t)$ is its partial derivative in time, $\mathbf{f} = \mathbf{f}(\mathbf{x}, t)$ is a known forcing function, F and G_1, \dots, G_n are (potentially nonlinear) spatial differential operators, and $\lambda_1, \dots, \lambda_n \in \mathbb{R}$ are fixed real numbers. Throughout the following we assume that solutions of (2.1) are classical [17], i.e., we will not concern ourselves with establishing the regularity of the solutions.

Motivated by [9, 18] and in tandem with (2.1), we consider the coupled system

$$(2.2) \quad \mathbf{v}_t + F(\mathbf{v}) + \sum_{k=1}^n \hat{\lambda}_k(t) G_k(\mathbf{v}) = \mathbf{f} + \mu(I_h(\mathbf{u}) - I_h(\mathbf{v})),$$

where $\hat{\lambda}_k(t)$ is the estimate for λ_k (which may evolve in time), I_h is a linear projection operator corresponding to partial observations of the true system state, and $\mu > 0$ is called the nudging parameter. The subscript h refers to the level of resolution of the projection (observation) operator, i.e. $h \rightarrow 0$ would indicate observation of all relevant scales. This is exactly the AOT formulation of [2], except that $\hat{\lambda}_k(t) \neq \lambda_k$, and these parameter estimates are updated along with the state estimate for \mathbf{v} . Our goal is to have $\mathbf{v}(t) \rightarrow \mathbf{u}(t)$ and $\hat{\lambda}_k(t) \rightarrow \lambda_k$ as $t \rightarrow \infty$. This requires an update formula for the $\hat{\lambda}_k(t)$, i.e., convergence of $\mathbf{v} \rightarrow \mathbf{u} + O(|\lambda_k - \hat{\lambda}_k(t)|)$ is guaranteed (under certain practical assumptions on (2.1)) following arguments similar to those put forward in [9, 18], but there is no immediately formulated update for $\hat{\lambda}_k(t)$ to guarantee that it approaches the true value λ_k .

In [9], two different update formulae are proposed for the 2D Navier-Stokes equations when the single unknown parameter λ is the viscosity of the system. Both approaches assume that $\mathbf{w} = \mathbf{u} - \mathbf{v}$ is sufficiently small so that quadratic terms can be neglected, leading to an update formula for $\hat{\lambda}(t)$. Such an assumption is valid, assuming that $\hat{\lambda}(t)$ is initially chosen close enough to λ so that \mathbf{w} is indeed small. Critically, this update formula is applicable only when $n = 1$, i.e. there is a single parameter to update.

2.1. Point-in-time Estimate. To motivate the update algorithm, we first consider (2.1) when both \mathbf{u} and \mathbf{u}_t are known exactly at a given time t , i.e., I_h is the identity operator. In this setting, the unknown parameters $\{\lambda_k(t)\}_{k=1}^n \subset \mathbb{R}$ can be recovered exactly at that time. Rearranging the original PDE (2.1) as

$$(2.3) \quad \sum_{k=1}^n \lambda_k G_k(\mathbf{u}) = \mathbf{f} - \mathbf{u}_t - F(\mathbf{u}),$$

we can obtain a system of scalar equations by taking inner products (duality pairing) with an ‘appropriate’ set of functions $\{\mathbf{e}_i\}_{i=1}^N \subset \mathcal{V}$:

$$(2.4) \quad \sum_{k=1}^n \lambda_k \langle \mathbf{e}_i, G_k(\mathbf{u}) \rangle = \langle \mathbf{e}_i, \mathbf{f} - \mathbf{u}_t - F(\mathbf{u}) \rangle,$$

for each $i = 1 \dots N$. So long as $\{G_k(\mathbf{u})\}_{k=1}^n$ is a linearly independent set, the above system can be solved uniquely to find the true parameters λ_k . The choice of the \mathbf{e}_i clearly influence the resultant linear system and play a critical role in the estimation of the λ_k . In practice, we desire to select the \mathbf{e}_i so that the linear system is well conditioned and hence numerical errors will not adversely affect the solution for the λ_k . The best way of selecting these functions to achieve this goal is not obvious, but one possibility is to choose an orthonormal set $\{\mathbf{e}_i\}_{i=1}^N$ so that at least the linear system is sampling from n different dimensions in the infinite-dimensional Hilbert space \mathcal{V} . We also note that we can select $N > n$ functions, in which case the linear system will be overdetermined and the λ_k may be found via linear regression. In practice we have not found this necessary and have always used $n = N$.

In practice, we only observe the projections $I_h(\mathbf{u})$ and $I_h(\mathbf{u}_t)$ (numerically this can be computed from $I_h(\mathbf{u})$ via finite differences since I_h is a linear operator) rather than \mathbf{u} and \mathbf{u}_t . To account for this, we apply I_h to both sides of (2.3), then take the inner product with each \mathbf{e}_i to reach an observable linear system:

$$(2.5) \quad \sum_{k=1}^n \lambda_k \langle \mathbf{e}_i, I_h(G_k(\mathbf{u})) \rangle = \langle \mathbf{e}_i, I_h(\mathbf{f} - \mathbf{u}_t - F(\mathbf{u})) \rangle.$$

Unfortunately, we cannot generically use $I_h(\mathbf{u})$ to compute $I_h(G_k(\mathbf{u}))$ or $I_h(F(\mathbf{u}))$, as it is not guaranteed that G_k or F commute with I_h . Motivated by the AOT formulation of this problem, we substitute \mathbf{v} for \mathbf{u} into the unknown terms, obtaining the system

$$(2.6) \quad \sum_{k=1}^n \hat{\lambda}_k \langle \mathbf{e}_i, I_h(G_k(\mathbf{v})) \rangle = \langle \mathbf{e}_i, I_h(\mathbf{f} - \mathbf{u}_t - F(\mathbf{v})) \rangle.$$

The solutions $\hat{\lambda}_1, \dots, \hat{\lambda}_n$ to this system are now only approximations of the true parameters, and the quality of this approximation depends on the estimated state \mathbf{v} being close to the true state \mathbf{u} , but as of yet we have not justified the assumption that $\mathbf{w} = \mathbf{u} - \mathbf{v}$ is small. The key is that, up to this point, we have placed no restrictions on the functions $\{\mathbf{e}_i\}_{i=1}^N$. We demonstrate next that choosing at least one of the \mathbf{e}_i carefully yields dynamical evidence (not yet rigorously justified) that $\mathbf{v} \rightarrow \mathbf{u}$, which consequently leads to the correct estimation of each λ_k as (2.6) synchronizes with (2.5).

2.2. Parameter Estimates as Control Parameters. From the previous discussion, we see that—at least morally—the convergence of the state \mathbf{v} to \mathbf{u} enables recovery of the true parameters. We now choose the \mathbf{e}_i to partially guarantee this convergence. As we will see in Section 3, this appears to work very well in practice.

Because I_h is linear and $\langle \cdot, \cdot \rangle$ is symmetric, $\frac{d}{dt} \|I_h(\mathbf{w})\|^2 = 2 \langle I_h(\mathbf{w}), I_h(\dot{\mathbf{w}}) \rangle$, where $\|\mathbf{u}\| = \sqrt{\langle \mathbf{u}, \mathbf{u} \rangle}$ is the norm induced by the inner product. Recalling $\mathbf{w} = \mathbf{u} - \mathbf{v}$ and

using (2.2),

$$\begin{aligned}
 (2.7) \quad \frac{d}{dt} \|I_h(\mathbf{w})\|^2 &= 2\langle I_h(\mathbf{w}), I_h(\mathbf{w}_t) \rangle \\
 &= 2\langle I_h(\mathbf{w}), I_h(\mathbf{u}_t) + I_h(F(\mathbf{v})) - I_h(\mathbf{f} + \mu I_h(\mathbf{w})) \rangle \\
 &\quad + 2 \sum_{k=1}^n \hat{\lambda}_k(t) \langle I_h(\mathbf{w}), I_h(G(\mathbf{v})) \rangle.
 \end{aligned}$$

Setting $\mathbf{e}_i = I_h(\mathbf{w})$ (or any multiple of $I_h(\mathbf{w})$) in (2.6) for some $i \in \{1, \dots, N\}$ yields

$$(2.8) \quad \sum_{k=1}^n \hat{\lambda}_k(t) \langle I_h(\mathbf{w}), I_h(G_k(\mathbf{v})) \rangle = \langle I_h(\mathbf{w}), I_h(\mathbf{f} - \mathbf{u}_t - F(\mathbf{v})) \rangle.$$

Combining (2.7) with (2.8), we find

$$\begin{aligned}
 \frac{1}{2} \frac{d}{dt} \|I_h(\mathbf{w})\|^2 &= \langle I_h(\mathbf{w}), I_h(\mathbf{u}_t) + I_h(F(\mathbf{v})) - I_h(\mathbf{f} + \mu I_h(\mathbf{w})) \rangle \\
 &\quad + \langle I_h(\mathbf{w}), I_h(\mathbf{f} - \mathbf{u}_t - F(\mathbf{v})) \rangle \\
 &= -\mu \langle I_h(\mathbf{w}), I_h(\mathbf{w}) \rangle \\
 &= -\mu \|I_h(\mathbf{w})\|^2.
 \end{aligned}$$

In this derivation we have used the linearity of I_h and the fact that I_h is a projection, i.e., $I_h(I_h(\mathbf{w})) = I_h(\mathbf{w})$. The final result is that the norm of the projected difference between the true solution \mathbf{u} and the nudged system \mathbf{v} decays to zero exponentially fast with rate μ . This is extremely promising, but we note that this does not automatically guarantee convergence of the parameter estimates, for two primary reasons: first, we do not have any guarantee that (2.6) has a solution; and second, although we formally have a guarantee of the convergence of $I_h(\mathbf{w}) \rightarrow 0$, this does not necessarily guarantee that $\mathbf{w} \rightarrow 0$ as well. Solvability of (2.6) appears to boil down to an appropriate choice of the other \mathbf{e}_i , and although we do not rigorously show that $I_h(\mathbf{w}) \rightarrow 0 \Rightarrow \mathbf{w} \rightarrow 0$, traditional Foias-Prodi type estimates typically used to guarantee convergence of AOT type algorithms apply in this setting with a correction term due to the differences in the truth λ_k and the estimate $\hat{\lambda}_k(t)$.

Correction terms for the differences between the two models are considered in a different context in both [9] and [18], although the current setting is far more general. The primary difficulty is that while this correction term is certainly estimable, it is updating in time, i.e. convergence of $\mathbf{w} \rightarrow 0$ is dependent on the convergence of $|\lambda_k - \hat{\lambda}_k(t)| \rightarrow 0$, and vice versa. That is, the dual convergence of the state and parameters can not be decoupled. This complicates the necessary estimates, although it certainly doesn't make them impossible. Further exploration is needed to provide a rigorous proof of this hypothesized convergence, although it does appear that such results are within reach.

A further complication is the choice of the other \mathbf{e}_i . That is, if we choose $\mathbf{e}_1 = I_h(\mathbf{w})$, how do we then select \mathbf{e}_i for $i > 1$? This introduces both theoretical and numerical/practical considerations. Theoretically, it may seem advantageous to choose \mathbf{e}_2 so that we can guarantee some higher order norm of $I_h(\mathbf{w})$ decays exponentially, much as was done above. However, it is not clear how to do this in practice, so we instead simply choose the \mathbf{e}_i to be orthonormal to obtain a well-conditioned linear system.

2.3. Numerical Considerations. As described above, we select $\mathbf{e}_1 = I_h(\mathbf{w})$ and choose the other \mathbf{e}_i to be orthonormal, ensuring that (2.6) is well conditioned. The straightforward approach is then to solve (2.6) at each timestep and use the obtained parameter estimates to advance \mathbf{v} . However, this is numerically problematic because it leads to rapid/discontinuous changes in the parameter at each time step. Such discontinuous adjustments quickly lead to numerical instabilities that are unavoidable if the update is applied at each time step, particularly when the initial parameter guess is not close to the predicted/true value.

To avoid discontinuous updates of the parameters $\hat{\lambda}_k(t)$, we numerically integrate

$$(2.10) \quad \frac{d\hat{\lambda}_k(t)}{dt} = -\alpha(\hat{\lambda}_k(t) - \tilde{\lambda}_k(t)),$$

where $\tilde{\lambda}_k(t)$ is obtained by solving (2.6) at each time t , and $\alpha > 0$ is a relaxation parameter. We then solve the coupled system given by (2.1)–(2.2) and (2.10). This gives a parameter update that avoids discontinuous changes in the parameters of the system, hence preserving the rigorously justified smoothness of the solutions \mathbf{v} and \mathbf{u} . The effect of the relaxation (finite values of α) are demonstrated in Figure 1 for KSE as described below.

Algorithm 2.1 details the entire parameter recovery procedure. Note that the algorithm is *concurrent* in the sense that the state estimates $\mathbf{v}_j := \mathbf{v}(t_j)$ can be computed as soon as the projected data at the corresponding time, $\hat{\mathbf{u}}_j := I_h(\mathbf{u}(t_j))$, becomes available. We denote this in the algorithm with the observation operator $\mathcal{Q} : t \mapsto I_h(\mathbf{u}(t))$. The state estimates are updated by time stepping (2.2), which we denote with a solution operator $\mathcal{S} : (\mathbf{v}_j, \hat{\lambda}_1, \dots, \hat{\lambda}_k) \mapsto \mathbf{v}_{j+1}$ with uniform time step $\delta t = t_{j+1} - t_j$.

Before presenting results of this parameter estimation strategy on KSE, we emphasize that the approach depends critically on assimilating data continuously in time so that the time derivative of the observed state $I_h(\mathbf{u}_t)$ can be approximated accurately. As shown in Figure 2, the error in the parameter approximation is directly dictated by this finite difference approximation, so that discrete measurements of $I_h(\mathbf{u})$ that are spaced too far apart in time will cause the parameter estimation to break down. All numerical results reported in Section 3 are based on continuous data assimilation in the sense that $I_h(\mathbf{u})$ is identified at every time step of the numerical solver.

3. Numerical Results. The non-dimensionalization of KSE that we consider has the following form:

$$(3.1) \quad u_t + u_{xxxx} + \lambda u_{xx} + uu_x = 0.$$

We impose periodic boundary conditions on the spatial domain $[0, 2\pi L)$. The chaos of the system depends on both λ and L . Higher values of L or λ increase the exhibited chaos [43, 26, 16, 13]. We choose $L = 16$, $\lambda = 1$ for all simulations as this represents a sufficiently chaotic state [28]. In all simulations, we use a Fourier collocation scheme with a fourth-order Runge-Kutta implicit-explicit time-stepper [29]. We note that the AOT nudging is applied via a forward Euler time-step to alleviate some concerns over the implicit nature of the RK method, and the parameter smoothing (2.10) is integrated via the trapezoid method for all simulations reported below. The number of Fourier collocation points is a minimum of 512 in each simulation, which guarantees that even the smallest scales are sufficiently resolved. The observation projection

Algorithm 2.1 Concurrent Multi-Parameter Estimation

```

1: procedure MPE( Initial time  $t_0 \in \mathbb{R}$ , time step  $\delta t > 0$ , projected state observer
    $\mathcal{Q} : \mathbb{R} \rightarrow \mathcal{V}$ , PDE solver  $\mathcal{S} : \mathcal{V} \times \mathbb{R}^n \rightarrow \mathcal{V}$  (time stepper), initial parameter
   guesses  $\hat{\lambda}_1, \dots, \hat{\lambda}_n \in \mathbb{R}$ , initial state estimate  $\mathbf{v}_0 \in \mathcal{V}$ , finite difference order  $p \in \mathbb{N}$ ,
   projector  $I_h : \mathcal{V} \rightarrow \mathcal{V}$ , nudging parameter  $\mu > 0$ , smoothing parameter  $\alpha > 0$  )
2:    $t \leftarrow t_0$ 
3:   for  $j = 0, 1, \dots$  do
4:     # Observe projected state and estimate its time derivative.
5:      $\hat{\mathbf{u}}_j \leftarrow \mathcal{Q}(t)$  # Projected state observation.
6:      $\hat{\mathbf{u}}'_j \leftarrow \text{BDF}(\hat{\mathbf{u}}_j, \dots, \hat{\mathbf{u}}_{j-p})$  # Backwards difference formula.
7:     # Construct and orthonormalize the basis vectors.
8:      $\mathbf{e}_1 \leftarrow \hat{\mathbf{u}}_j - I_h(\mathbf{v}_j)$ 
9:     for  $k = 2, \dots, n$  do
10:       $\mathbf{e}_k \leftarrow I_h(G_{k-1}(\mathbf{v}_j))$ 
11:      $\mathbf{e}_1, \dots, \mathbf{e}_n \leftarrow \text{MGS}(\mathbf{e}_1, \dots, \mathbf{e}_n)$  # Modified Gram-Schmidt.
12:     # Construct system for estimating parameters.
13:      $\mathbf{b} \in \mathbb{R}^n, \mathbf{A} \in \mathbb{R}^{n \times n}$  # Initialize empty n x n linear system.
14:     for  $k = 1, \dots, n$  do
15:        $b_k \leftarrow \langle \mathbf{e}_k, \mathbf{f} - \hat{\mathbf{u}}'_j - I_h(F(\mathbf{v}_j)) \rangle$ 
16:       for  $\ell = 1, \dots, n$  do
17:          $A_{k,\ell} \leftarrow \langle \mathbf{e}_k, I_h(G_\ell(\mathbf{v}_j)) \rangle$ 
18:     # Get point-in-time estimates and smooth.
19:      $\tilde{\lambda}_1, \dots, \tilde{\lambda}_n \leftarrow \mathbf{A}^{-1}\mathbf{b}$ 
20:     for  $k = 1, \dots, n$  do
21:        $\hat{\lambda}_k \leftarrow (1 + \frac{1}{2}\alpha\delta t)^{-1} \left[ (1 - \frac{1}{2}\alpha\delta t) \hat{\lambda}_k + \alpha\delta t \tilde{\lambda}_k \right]$ 
22:     # Update estimated state with AOT nudging.
23:      $\mathbf{v}_{j+1} \leftarrow \mathcal{S}(\mathbf{v}_j, \hat{\lambda}_1, \dots, \hat{\lambda}_n) + \mu\delta t(\hat{\mathbf{u}}_j - I_h(\mathbf{v}_j))$ 
24:      $t \leftarrow t + \delta t$ 
25:   return  $\hat{\lambda}_1, \dots, \hat{\lambda}_n$ 

```

operator is a Galerkin truncation onto the lowest 21 modes, meaning that $h \approx \frac{32\pi}{21}$ for all computations reported below. All simulations are run out from $t = 0$ to at least $t_f = 50$ in non-dimensional units. The code for running the simulations and generating the figures in this paper is publicly available at <https://github.com/Parametric-Data-Assimilation/kse-parameter-estimation>.

3.1. Single-parameter Estimation. We begin with a discussion of the performance of our algorithm when estimating a single unknown parameter λ , i.e.,

$$(3.2a) \quad u_t + u_{xxxx} + \lambda u_{xx} + uu_x = 0, \quad (\text{truth})$$

$$(3.2b) \quad v_t + v_{xxxx} + \hat{\lambda} v_{xx} + vv_x = \mu(I_h(u) - I_h(v)), \quad (\text{assim})$$

denoting v for the nudging variable. In general, we observe the expected exponential decay of the projected error in time as demonstrated in Figure 1. Defining $w := u - v$, both the solution error $\|w\|$ and error in the parameter $|\lambda - \hat{\lambda}|$ exhibit corresponding exponential decay. The rate of this decay (or convergence rate) depends on the

parameters μ for the data assimilation and α for the parameter update. Increasing either μ or α will lead to faster convergence, but extreme values of either parameter can violate the numerical stability criteria of the selected time-stepping scheme. The natural scaling for μ is with δt^{-1} (the inverse of the timestep). The stability region of a simple nudging as applied here indicates that $\mu \geq 2\delta t^{-1}$ leads to instability, so we take $\mu = 1.8\delta t^{-1}$ in all experiments.

3.1.1. The Effect of the Smoothing Parameter. For single-parameter estimation, the algorithm converges without relaxation of the parameter estimates, i.e., $\alpha = \infty$. However, the convergence is smoother when relaxation is used, at the cost of a slower convergence rate (see Figure 1). Although numerical stability of the time stepping scheme allows for $\alpha \sim \delta t^{-1}$, we find that $\alpha \gg 1$ is essentially equivalent to no relaxation. Hence, in all that follows, we set $\alpha = 1$.

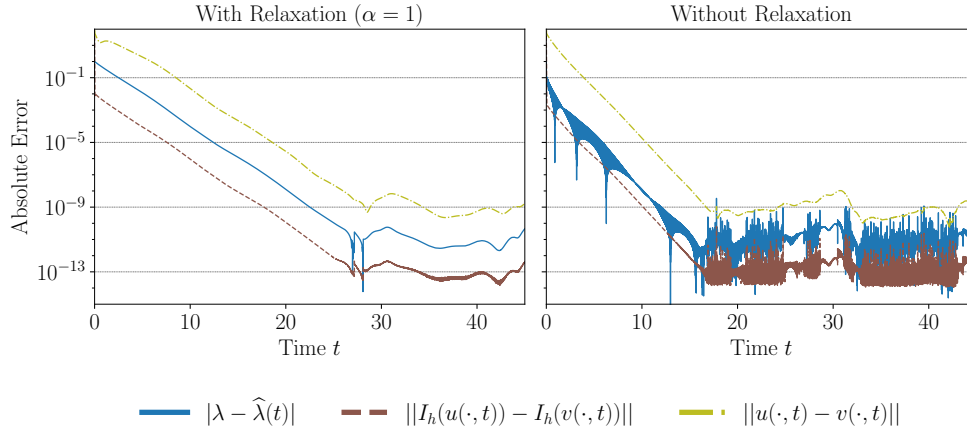


Fig. 1: The effect of finite relaxation (specifically $\alpha = 1$) on convergence.

3.1.2. Order of Accuracy. The accuracy of the parameter estimate, and hence the estimate of the solution u , is limited by three factors: 1) the error introduced by the numerical scheme for the PDE, 2) round-off error, and 3) errors introduced by finite difference estimates of $I_h(u_t)$. Of these factors, the finite difference error for estimating $I_h(u_t)$ is the most significant, and therefore the order of the corresponding finite difference scheme controls the order of accuracy for the final parameter estimate (with respect to δt). Figure 2 shows the final error in the parameter estimate with respect to δt for different backward differencing methods used to estimate $I_h(u_t)$ (we use only backward differencing as only previous time step data is available to us). We note that errors from the underlying PDE solver, and particularly the data assimilation aspect of the time stepping with the Runge-Kutta scheme (see [18] for a description of this kind of error in a different setting, and [38] for a more thorough discussion of this issue) limit the overall error to approximately 10^{-12} , which is seen by the saturation of the error for both the 2nd- and 3rd-order finite difference methods in Figure 2. Omitting these final points, we obtain a linear regressed exponent that fits nearly exactly with the order of the finite difference method for the temporal derivative. As these numerical investigations are meant to provide a proof of concept only, the error introduced via the RK time stepping is an acceptable compromise to

the ease of implementation and accessibility of the code.

We consider the propagation of the error in the 3rd-order backwards difference method specifically to understand the increase in the parameter error for $\delta t < 10^{-3}$. If we allow ξ to be the error from the Runge-Kutta time-stepping in the data assimilation step, then the numerically ‘converged’ state of the system should be $\tilde{I}_h(u) \approx I_h(u) + \xi$, where $\xi = \xi(\delta t, N, \epsilon_{\text{machine}})$ is a function of the time step size, number of collocation points N , and machine epsilon $\epsilon_{\text{machine}}$. Using a 3rd-order backward difference to approximate $I_h(u_t)$ in this case leads to

$$\tilde{I}_h(u_t) \approx I_h(u_t) + \frac{\xi}{\delta t} + O(\delta t^3).$$

The problem is that, as noted in [18] in a different setting, the multi-stage Runge-Kutta method introduces an error $\xi > \epsilon_{\text{machine}}$ independent of δt itself. Thus, there is a certain point at which decreasing δt counterintuitively leads to increased error in $\tilde{I}_h(u_t)$, and hence an increased error in the parameter estimation. The rub of the matter is that the two smallest values of δt for the 3rd-order difference are purely artifacts of the RK time stepping, and are hence numerically irrelevant to a discussion on the order of convergence.

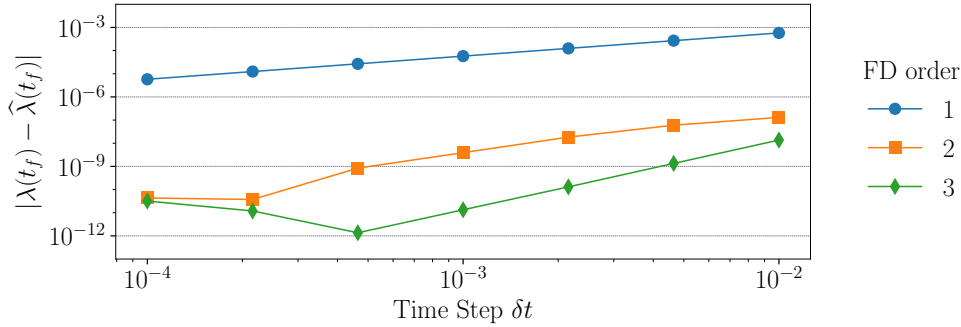


Fig. 2: Log-log plot of parameter error with respect to δt for finite difference methods of order 1, 2, and 3. Using the indicated points, the order of the parameter estimation error is calculated via linear regression as 1.0003, 1.95, and 3.002 respectively (for the third-order method we exclude the last two points). Excluding the last point for the second-order method gives an order of 2.05.

3.2. Multi-parameter Estimation. The primary contribution of the algorithm presented here is the ability to learn multiple unknown parameters in a single equation in a concurrent fashion. To this end, we consider a *generalized KSE* for the assimilated system $v(x, t)$, defined as

$$(3.3a) \quad u_t + \lambda_4 u_{xxxx} + \lambda_2 u_{xx} + \lambda_5 u u_x = 0, \quad (\text{truth})$$

$$(3.3b) \quad v_t + \hat{\lambda}_4 v_{xxxx} + \hat{\lambda}_3 v_{xxx} + \hat{\lambda}_2 v_{xx} + \hat{\lambda}_1 v_x + \hat{\lambda}_5 v v_x = \mu(I_h(u) - I_h(v)). \quad (\text{assim})$$

Once again we will consider $x \in [0, 2\pi L)$ with $L = 16$ fixed in these simulations. We will run all simulations from time $t = 0$ to $t_f = 50$. Following the discussion above for the single parameter case, we will consider only $\delta t = 10^{-3}$ with the 3rd-order backward differencing approximation to the temporal derivative.

The goal of this investigation is not only to identify the correct parameters of the specified PDE, but also to allow discover the structure of an unknown equation. Hence, we have expanded the standard KSE to include unknown parameters on all terms and additional parameters on linear odd-order derivatives. The true KSE corresponds to the case when $\lambda_1 = \lambda_3 = 0$ and $\lambda_2 = \lambda_4 = \lambda_5 = 1$. We investigate whether the algorithm developed here can recover these values. In each experiment, we choose a subset of the λ_k to learn, and set the rest to their true values (from (3.3a)). The simulation is initialized with an initial guess of $\hat{\lambda}_k = 2$ for every k that is to be learned.

Before presenting our numerical results, we discuss a few of the implementation details which are not obvious from the theoretical derivation of the algorithm.

3.2.1. Choice of Basis. A crucial piece of the algorithm is the choice of basis functions e_1, \dots, e_N . Other than setting $e_1 = I_h(w)$ (to ensure exponential decay of $I_h(w)$ in L^2), it is not clear how to choose these functions. For efficiency, we would like to use information that is already available. A natural choice is then to use the $I_h(G_k(v))$, as these are computed in the simulation itself. Here another ambiguity arises—we need only $n - 1$ more basis elements, but there are n of the $I_h(G_k(v))$, hence we may exclude one. Most of the time, the choice does not affect convergence. However, we find that when G_k corresponds to the nonlinear term in the generalized KSE, including it as a basis element causes the algorithm to not converge. Consequently, we always exclude this term from the basis.

For numerical stability, the basis vectors are orthonormalized before constructing the system (2.5). While it is technically possible for the system to be degenerate, we do not observe this in practice. In addition, orthonormalizing the basis vectors eliminates potential near-degeneracies which are likely in such a high-dimensional space.

3.2.2. Convergence. As for the case of single-parameter estimation, we observe exponential convergence in time to the true parameters in the multi-parameter case. However, there are additional limitations when multiple parameters are considered. When estimating multiple unknown parameters, the point-in-time estimates must be smoothed or the algorithm will fail to converge, i.e. the rapid changes in parameter values introduce non-physical discontinuous features and reactions to the system which overwhelm the continuous data assimilation. Additionally, not every combination of unknown parameters can be learned (at least based on the experiments considered here). In particular, we find that λ_5 (the coefficient for the nonlinear term) cannot be learned at the same time as λ_1 or λ_3 —both of which are equal to 0 in the true KSE. Every other combination of unknown parameters can be successfully recovered. It appears that this approach can either recover the nonlinear dynamics, or it can perform model discovery, but not both simultaneously.

Estimation of the coefficients of the linear terms $\lambda_1, \lambda_2, \lambda_3$, and λ_4 is very efficient and appears to work down to an error of $O(10^{-11})$, consistent with our previous results when recovering a single parameter. See Figure 3 for a convergence plot for an estimation of all four linear-term coefficients. Note that the convergence rate is very similar to that observed for the single parameter case (see the left part of Figure 1). It also appears that estimation of the dissipative coefficients ($k = 2, 4$) behaves similarly, while the dispersive terms ($k = 1, 3$) also converge in a similar fashion (smoother than the dissipative ones). This could either be a product of the differences between dispersion and dissipation, or it may be simply because $\lambda_1 = \lambda_3 = 0$ in the true system.

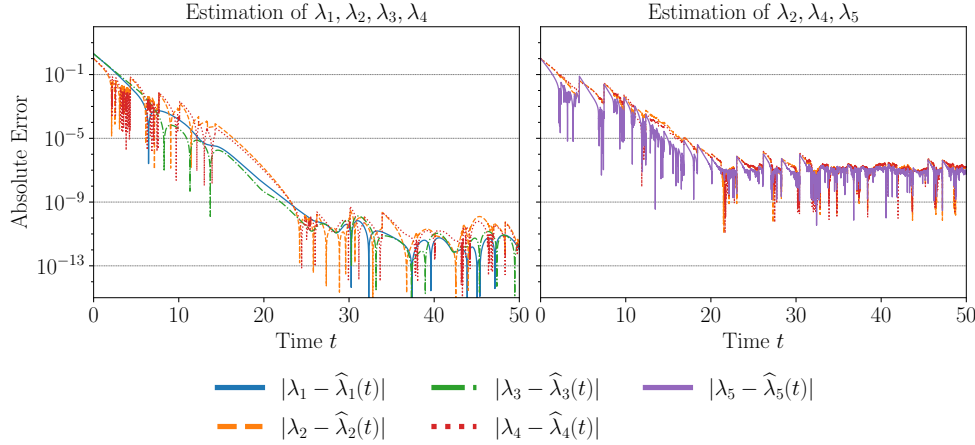


Fig. 3: Convergence of multi-parameter estimation with respect to time for the four parameters corresponding to linear terms in the generalized KSE (3.3b) (left) and for the three parameters corresponding to terms in the original KSE, including the nonlinear coefficient (right).

Complete parameter recovery without the addition of the dispersive $k = 1, 3$ terms, but including the nonlinear term, is also demonstrated in Figure 3. Note that the final ‘converged’ error in this case is significantly worse, appearing to level off at $O(10^{-7})$ for all parameters, even though the convergence rate is very similar (the error stops decreasing at about the same time). It is not immediately clear why this combination of coefficients does not achieve the same level of accuracy, but it appears that the unknown coefficient on the nonlinearity plays a pivotal role. Even with this decrease in final accuracy, recovery of the true parameters up to $O(10^{-7})$ for such a concurrent learning algorithm is significant.

It is worth mentioning that the algorithm experiences no loss of accuracy when λ_5 is the single unknown parameter (see Figure 4). Decrease in accuracy only arises when estimating λ_5 in tandem with other unknown parameters.

Our experiments indicate that the method appears to be robust to changes in the values of α and/or the initial values of the parameters, i.e., we may make a choice other than $\hat{\lambda}_k(0) = 2$. On the contrary, the choice of the basis functions $\{e_i\}_{i=1}^N$ is critical: failing to include the error term e_1 and instead using basis functions corresponding to the first n Fourier modes leads to a failure to converge. We also attempted estimating the parameters at each time-step via a least-squares fit using several additional basis functions (N total), as opposed to exactly solving a small linear system. This led to similar convergence to the method presented in detail here, but at increased computational expense. Furthermore, the theoretical justification is less clear for this alternate method, so we leave a more detailed investigation of this and other alternative basis functions to a later study.

4. Conclusions. We have developed an algorithm for concurrently learning parameters and assimilating the state in a general setting for evolutionary, dissipative PDEs, and shown that it works remarkably well on a generalized version of the Kuramoto-Sivashinsky equation. Numerically, we observe that multiple parameters

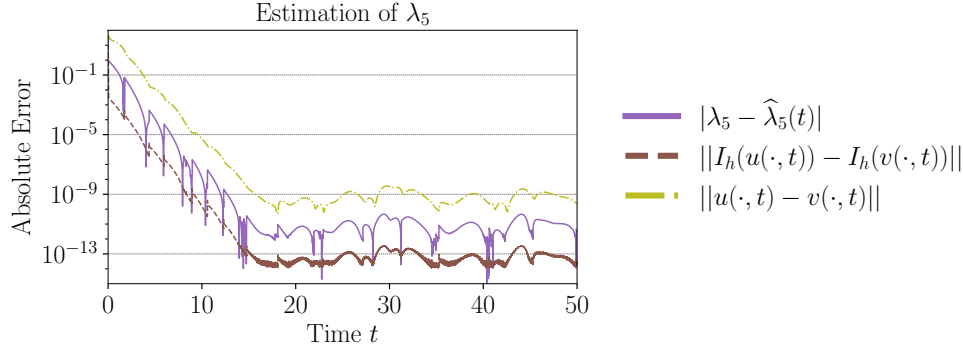


Fig. 4: Convergence of single-parameter estimation with respect to time for the parameter corresponding to the nonlinear term only in the KSE, as well as the state and projected state error.

(coefficients) of KSE can be recovered up to an explainable error (due to the RK time stepping and data assimilation method) so long as these parameters are coefficients on linear terms in the equation. We have also demonstrated that the coefficient of the nonlinear term can be recovered, but only in concert with dissipative linear terms and then at a significant cost to the final error. Essentially, although there are limitations to the developed approach, it is shown to work remarkably well on KSE.

Further applications of this algorithm are readily apparent. Parameter learning or model recovery for physically motivated systems are interesting and well-motivated problems. Although the derivation in [Section 2](#) is not rigorous, it does appear that this approach will work for all dissipative systems for which the AOT algorithm has been shown to converge, which represents a very large class of PDEs. Extensions beyond the simplified setting where the ‘true’ system is run simultaneously as a direct numerical simulation are of greater interest and will be explored at length. For instance, a lofty extension of this work would be to estimate the skin friction of a surface from data collected via wind tunnel experiments. Such an application of this approach of course entails additional complications that have not been considered here.

On a related note, the derivation provided here is intuitive, but certainly not completely rigorous. We have not provided rigorous justification for the observed convergence of both the parameter learning and the convergence of the state. The rigorous justification of this algorithm for certain systems of PDEs will not only provide a firm mathematical foundation for this effort, but will also highlight the necessary hypotheses on the hyperparameters (level of projection h , etc.) that will guide the practical implementation of this method in other settings.

Appendix A. Numerical Solution to the Generalized KSE. This section provides essential details on the KSE numerical solver.

We consider a generalized version of KSE,

$$u_t + \lambda_1 u_x + \lambda_2 u_{xx} + \lambda_3 u_{xxx} + \lambda_4 u_{xxxx} + \lambda_5 uu_x = 0.$$

The classical KSE has $\lambda_1 = \lambda_3 = 0$. Let \mathcal{F} denote the Fourier transform and denote $\hat{u}(\xi, t) = [\mathcal{F}(u(\cdot, t))](\xi)$. Recall $[\mathcal{F}(\frac{d^k}{dx^k} \phi)](\xi) = (2\pi i \xi)^k [\mathcal{F}(\phi)](\xi)$. Taking the Fourier transform of both sides of the generalized KSE we arrive at the spectral version of

the PDE,

$$\hat{u}_t + \lambda_1(2\pi i\xi)\hat{u} + \lambda_2(2\pi i\xi)^2\hat{u} + \lambda_3(2\pi i\xi)^3\hat{u} + \lambda_4(2\pi i\xi)^4\hat{u} + \lambda_5\mathcal{F}(uu_x) = 0.$$

To elucidate the numerical implementation of this equation, we let \mathcal{F}^{-1} denote the inverse Fourier transform, i.e. $u(x, t) = \mathcal{F}^{-1}(\hat{u})$. This immediately yields the standard pseudo-spectral scheme:

$$\begin{aligned} \hat{u}_t = & - \left[\lambda_1(2\pi i\xi) + \lambda_2(2\pi i\xi)^2 + \lambda_3(2\pi i\xi)^3 + \lambda_4(2\pi i\xi)^4 \right] \hat{u} \\ & - \lambda_5 \mathcal{F} \left(\mathcal{F}^{-1}(\hat{u}) \mathcal{F}^{-1}(2\pi i\xi \hat{u}) \right). \end{aligned}$$

The primary remaining aspects of the numerical scheme are then the choice of a time-stepping discretization of \hat{u}_t , and the finite truncation level of the Fourier transform.

All the simulations performed here are done with an implicit-explicit Runge-Kutta 4-stage method that is formally 4th order, and the Fourier series are all truncated with $N = 512$ spatial points. We also implement a 2/3 dealiasing to avoid unnecessary overflow to the smallest scales. The choice of domain size and the value of $\lambda_1 = 1$ is selected for this degree of spatial resolution because even when dealiasing is removed, the power spectrum of the simulation is fully resolved with these parameters, i.e., the magnitude of the smallest-scale terms is near $\epsilon_{\text{machine}}$.

For the data assimilation step, the projection operator $I_h(u)$ is simply defined by zeroing out all modes with wave numbers greater than a cutoff K selected as $K = 21$ in everything presented here. All simulations for the true state are started with initial condition

$$\begin{aligned} u_0(x) = & \sin\left(6\frac{\pi x}{L}\right) + 0.1 \cos\left(\frac{\pi x}{L}\right) - 0.2 \sin\left(3\frac{\pi x}{L}\right) \\ & + 0.05 \cos\left(15\frac{\pi x}{L}\right) + 0.7 \sin\left(18\frac{\pi x}{L}\right) - \cos\left(13\frac{\pi x}{L}\right), \end{aligned}$$

and then run out to non-dimensional time $\tilde{t} = 10$ whereupon the assimilated system is initialized.

Acknowledgments. The authors would like to thank E. Carlson, J. Hudson, A. Larios, V. Martinez, and E. Ng for their helpful discussions. JPW was partially supported by the Simons Foundation travel grant 586788.

REFERENCES

- [1] A. AZOUANI, E. OLSON, AND E. S. TITI, *Continuous data assimilation using general interpolant observables*, Journal of Nonlinear Science, 24 (2014), pp. 277–304.
- [2] A. AZOUANI, E. OLSON, AND E. S. TITI, *Continuous data assimilation using general interpolant observables*, Journal of Nonlinear Science, 24 (2014), pp. 277–304.
- [3] H. BESSAIH, E. OLSON, AND E. S. TITI, *Continuous data assimilation with stochastically noisy data*, Nonlinearity, 28 (2015), p. 729.
- [4] A. BISWAS, Z. BRADSHAW, AND M. S. JOLLY, *Data assimilation for the Navier-Stokes equations using local observables*, arXiv preprint arXiv:2008.06949, (2020).
- [5] A. BISWAS, J. HUDSON, A. LARIOS, AND Y. PEI, *Continuous data assimilation for the 2D magnetohydrodynamic equations using one component of the velocity and magnetic fields*, Asymptotic Analysis, 108 (2018), pp. 1–43.
- [6] J. BORGGAARD, N. GLATT-HOLTZ, AND J. KROMETIS, *A Bayesian approach to estimating background flows from a passive scalar*, SIAM/ASA Journal on Uncertainty Quantification, 8 (2020), pp. 1036–1060.
- [7] S. L. BRUNTON, J. L. PROCTOR, AND J. N. KUTZ, *Discovering governing equations from data by sparse identification of nonlinear dynamical systems*, Proceedings of the National Academy of Sciences, 113 (2016), pp. 3932–3937.

- [8] N. B. BUDANUR AND P. CVITANOVIĆ, *Unstable manifolds of relative periodic orbits in the symmetry-reduced state space of the Kuramoto–Sivashinsky system*, Journal of Statistical Physics, 167 (2017), pp. 636–655.
- [9] E. CARLSON, J. HUDSON, AND A. LARIOS, *Parameter recovery for the 2 dimensional Navier–Stokes equations via continuous data assimilation*, SIAM Journal on Scientific Computing, 42 (2020), pp. A250–A270.
- [10] E. CARLSON, J. HUDSON, A. LARIOS, V. R. MARTINEZ, E. NG, AND J. P. WHITEHEAD, *Parameter learning for the Lorenz equation via controlled data assimilation*, in preparation, (2021).
- [11] B. I. COHEN, J. KROMMES, W. TANG, AND M. ROSENBLUTH, *Non-linear saturation of the dissipative trapped-ion mode by mode coupling*, Nuclear Fusion, 16 (1976), p. 971.
- [12] P. COLLET, J.-P. ECKMANN, H. EPSTEIN, AND J. STUBBE, *A global attracting set for the Kuramoto–Sivashinsky equation*, Communications in mathematical physics, 152 (1993), pp. 203–214.
- [13] P. CVITANOVIĆ, R. L. DAVIDCHACK, AND E. SIMINOS, *On the state space geometry of the Kuramoto–Sivashinsky flow in a periodic domain*, SIAM Journal on Applied Dynamical Systems, 9 (2010), pp. 1–33.
- [14] M. DASHTI AND A. M. STUART, *The Bayesian approach to inverse problems*, Handbook of Uncertainty Quantification, (2016), pp. 1–118.
- [15] P. C. DI LEONI, A. MAZZINO, AND L. BIFERALE, *Inferring flow parameters and turbulent configuration with physics-informed data assimilation and spectral nudging*, Physical Review Fluids, 3 (2018), p. 104604.
- [16] R. A. EDSON, J. E. BUNDER, T. W. MATTNER, AND A. J. ROBERTS, *Lyapunov exponents of the Kuramoto–Sivashinsky PDE*, ANZIAM Journal, 61 (2019), pp. 270–285.
- [17] L. C. EVANS, *Partial differential equations*, Graduate studies in mathematics, 19 (1998).
- [18] A. FARHAT, N. GLATT-HOLTZ, V. R. MARTINEZ, S. A. MCQUARRIE, AND J. P. WHITEHEAD, *Data assimilation in large Prandtl Rayleigh–Bénard convection from thermal measurements*, SIAM Journal on Applied Dynamical Systems, 19 (2020), pp. 510–540.
- [19] A. FARHAT, H. JOHNSTON, M. JOLLY, AND E. S. TITI, *Assimilation of nearly turbulent Rayleigh–Bénard flow through vorticity or local circulation measurements: A computational study*, Journal of Scientific Computing, (2017), pp. 1–15.
- [20] A. FARHAT, M. S. JOLLY, AND E. S. TITI, *Continuous data assimilation for the 2D Bénard convection through velocity measurements alone*, Physica D: Nonlinear Phenomena, 303 (2015), pp. 59–66.
- [21] A. FARHAT, E. LUNASIN, AND E. S. TITI, *Abridged continuous data assimilation for the 2D Navier–Stokes equations utilizing measurements of only one component of the velocity field*, Journal of Mathematical Fluid Mechanics, 18 (2016), pp. 1–23.
- [22] A. FARHAT, E. LUNASIN, AND E. S. TITI, *On the Charney conjecture of data assimilation employing temperature measurements alone: the paradigm of 3D planetary geostrophic model*, Mathematics of Climate and Weather Forecasting, 1 (2016).
- [23] C. FOIAS, G. R. SELL, AND E. S. TITI, *Exponential tracking and approximation of inertial manifolds for dissipative nonlinear equations*, Journal of Dynamics and Differential Equations, 1 (1989), pp. 199–244.
- [24] D. GOLUSKIN AND G. FANTUZZI, *Bounds on mean energy in the Kuramoto–Sivashinsky equation computed using semidefinite programming*, Nonlinearity, 32 (2019), p. 1705.
- [25] Z. GRUJIĆ, *Spatial analyticity on the global attractor for the Kuramoto–Sivashinsky equation*, Journal of Dynamics and Differential Equations, 12 (2000), pp. 217–228.
- [26] J. M. HYMAN AND B. NICOLAENKO, *The Kuramoto–Sivashinsky equation: a bridge between PDE’s and dynamical systems*, Physica D: Nonlinear Phenomena, 18 (1986), pp. 113–126.
- [27] M. S. JOLLY, V. R. MARTINEZ, AND E. S. TITI, *A data assimilation algorithm for the subcritical surface quasi-geostrophic equation*, Advanced Nonlinear Studies, 17 (2017), pp. 167–192.
- [28] A.-K. KASSAM AND L. N. TREFETHEN, *Fourth-order time-stepping for stiff PDEs*, SIAM Journal on Scientific Computing, 26 (2005), pp. 1214–1233.
- [29] C. A. KENNEDY AND M. H. CARPENTER, *Additive Runge–Kutta schemes for convection–diffusion–reaction equations*, Applied Numerical Mathematics, 44 (2003), pp. 139–181.
- [30] Y. KURAMOTO AND T. TSUZUKI, *On the formation of dissipative structures in reaction-diffusion systems: Reductive perturbation approach*, Progress of Theoretical Physics, 54 (1975), pp. 687–699.
- [31] R. E. LAQUEY, S. MAHAJAN, P. RUTHERFORD, AND W. TANG, *Nonlinear saturation of the trapped-ion mode*, Physical Review Letters, 34 (1975), p. 391.
- [32] A. LARIOS AND Y. PEI, *Nonlinear continuous data assimilation*, arXiv preprint

- arXiv:1703.03546, (2017).
- [33] Z. LI, N. KOVACHKI, K. AZIZZADENESHELI, B. LIU, K. BHATTACHARYA, A. STUART, AND A. ANANDKUMAR, *Fourier neural operator for parametric partial differential equations*, arXiv preprint arXiv:2010.08895, (2020).
 - [34] E. N. LORENZ, *Deterministic nonperiodic flow*, Journal of the Atmospheric Sciences, 20 (1963), pp. 130–141.
 - [35] L. LU, P. JIN, AND G. E. KARNIADAKIS, *DeepOnet: Learning nonlinear operators for identifying differential equations based on the universal approximation theorem of operators*, arXiv preprint arXiv:1910.03193, (2019).
 - [36] C. MISBAH AND A. VALANCE, *Secondary instabilities in the stabilized Kuramoto-Sivashinsky equation*, Physical Review E, 49 (1994), p. 166.
 - [37] B. NICOLAENKO, B. SCHEURER, AND R. TEMAM, *Some global dynamical properties of the Kuramoto-Sivashinsky equations: nonlinear stability and attractors*, Physica D: Nonlinear Phenomena, 16 (1985), pp. 155–183.
 - [38] E. OLSON AND E. S. TITI, *Determining modes and Grashof number in 2D turbulence: A numerical case study*, Theoretical and Computational Fluid Dynamics, 22 (2008), pp. 327–339.
 - [39] M. QUADE, M. ABEL, J. NATHAN KUTZ, AND S. L. BRUNTON, *Sparse identification of nonlinear dynamics for rapid model recovery*, Chaos: An Interdisciplinary Journal of Nonlinear Science, 28 (2018), p. 063116.
 - [40] M. RAISSI, P. PERDIKARIS, AND G. KARNIADAKIS, *Physics-informed neural networks: A deep learning framework for solving forward and inverse problems involving nonlinear partial differential equations*, Journal of Computational Physics, 378 (2019), pp. 686–707.
 - [41] G. SIVASHINSKY, *Nonlinear analysis of hydrodynamic instability in laminar flames—I. Derivation of basic equations*, Acta Astronautica, 4 (1977), pp. 1177–1206.
 - [42] G. I. SIVASHINSKY AND D. MICHELSON, *On irregular wavy flow of a liquid film down a vertical plane*, Progress of Theoretical Physics, 63 (1980), pp. 2112–2114.
 - [43] R. W. WITTENBERG AND P. HOLMES, *Scale and space localization in the Kuramoto-Sivashinsky equation*, Chaos: An Interdisciplinary Journal of Nonlinear Science, 9 (1999), pp. 452–465.